How should we sample snail microbiomes?

Lauren V. Carruthers[1], Stephanie C. Nordmeyer[2], Timothy JC. Anderson[2], Frédéric D. Chevalier[2¶*], Winka Le Clec'h[2¶*]

1. School of Infection and Immunity, University of Glasgow, Glasgow G12 8TA, UK.
2. Texas Biomedical Research Institute, PO Box 760549, San Antonio, TX 78258.

Author information:

- Lauren V. Carruthers: Lauren.Carruthers@glasgow.ac.uk – ORCID: 0000-0003-4346-2283
- Stephanie C. Nordmeyer: SNordmeyer@txbiomed.org – ORCID: 0000-0003-3847-3498
- Timothy JC. Anderson: tanderso@txbiomed.org – ORCID: 0000-0002-0191-0204
- Frédéric D. Chevalier*: fcheval@txbiomed.org – ORCID: 0000-0003-2611-8106
- Winka Le Clec'h*: winkal@txbiomed.org – ORCID: 0000-0002-1111-2492

¶ Equally contributed

* Corresponding authors

Running title: How should we sample snail microbiomes?

ABSTRACT

Background: The microbiome is increasingly recognized to shape many aspects of its host biology and is a key determinant of health and disease. The microbiome may influence transmission of pathogens by their vectors, such as mosquitoes or aquatic snails. We previously sequenced the bacterial 16S V4 ribosomal DNA of the hemolymph (blood) of *Biomphalaria* spp. snails, one of the vectors of the human blood fluke schistosome. We showed that snail hemolymph harbored an abundant and diverse microbiome. This microbiome is distinct from the water environment and can discriminate snail species and populations. As hemolymph bathes snail organs, we then investigated the heterogeneity of the microbiome in these organs.

Results: We dissected ten snails for each of two different species (*B. alexandrina* and *B. glabrata*) and collected their organs (ovotestis, hepatopancreas, gut, and stomach). We also ground in liquid nitrogen four whole snails of each species. We sampled the water in which the snails were living (environmental controls). Sequencing the 16S V4 rDNA revealed organ-specific microbiomes. These microbiomes harbored a lower diversity than the hemolymph microbiome, and the whole-snail microbiome. The organ microbiomes tend to cluster by physiological function. In addition, we showed that the whole-snail microbiome is more similar to hemolymph microbiome.

Conclusions: These results are critical for future work on snail microbiomes and show the necessity of sampling individual organ microbiomes to provide a complete description of snail microbiomes.

Keywords: Microbiome, organs, tissues, *Biomphalaria* snails, 16S rDNA.

INTRODUCTION

Over the past decade, the microbiomes of both vertebrate and invertebrate hosts have been extensively characterized [1,2] and are recognized to shape many aspects of their host biology, health, and evolution [3,4]. As sequencing costs are decreasing, it is now affordable to investigate the microbiomes at the organ or tissue scale. While this is now routine for vertebrate microbiomes, microbiome studies of invertebrates are often limited to the whole body, especially for small invertebrates (e.g., flies, mosquitoes, snails). Using whole-body microbiome however, can mask organ-specific and important microbiome features due to its composite nature. Additionally, changes in microbiome composition can be obscured at the whole-body level. This issue shares similarities with challenges encountered in other fields of systems biology, such as cancer and immunology. For instance, the progress made from analyzing gene expression at bulk levels to single-cell levels has significantly transformed our understanding of biology and medicine [5,6]. To increase the resolution of microbiome studies, it is preferable to focus on organ or tissue-specific microbiomes rather than whole-body microbiomes. This approach has already been applied to invertebrate organisms, such as marine mollusks - oysters, mussels, and clams [7–9] - and terrestrial crustaceans [10,11].

Biomphalaria snails are freshwater mollusks and vectors of several trematode species, including the human blood fluke schistosome. Schistosomes infect over 200 million people in 78 countries in tropical and subtropical regions, with schistosomiasis responsible for over 200,000 estimated deaths annually [12–14]. Like many other marine and freshwater mollusks, *Biomphalaria* snails harbor a diverse microbiome in their hemolymph [15]. Since hemolymph bathes snail organs, our study aimed to investigate the composition of the microbiome of these organs.

We therefore profiled the microbiome of multiple organs and tissues (hemolymph, stomach, gut, hepatopancreas (i.e. liver), and ovotestis) from two *Biomphalaria* species: *B.*

glabrata, native to Brazil, and *B. alexandrina*, native to Egypt. We compared these specific organ microbiome profiles to whole-snail microbiomes, as well as the microbiomes found in the snail's environmental water. Our findings demonstrate that the overall snail microbiome is not a true composite of the microbiomes of its various organs and is actually more similar to the hemolymph and, like the hemolymph, contains a highly diverse microbial community. Interestingly, we observed that the type of organ or tissue is the primary factor shaping the microbiome, rather than the snail species.

Our study highlights the importance of a well-thought-out sampling strategy when studying the snail microbiome. Both hemolymph and whole-snail samples capture a high microbiome diversity, but not in the same way. Conversely, the gut and stomach exhibited the highest microbiome density of all organs. Therefore, tailoring the sampling approach to the specific research question is crucial to provide the most accurate answer and avoid masking the effect of specific or rare taxa when analyzing the snail microbiome.

MATERIALS AND METHODS

1. *Biomphalaria spp.* snail culture.

Biomphalaria alexandrina and *B. glabrata* BS90 snails were reared separately in 10-gallon tanks containing aerated freshwater (sourced from a well on site at Texas Biomedical Research Institute) at 26-28°C on a 12-hour light – 12-hour dark photocycle. They were fed *ad libitum* with green leaf lettuce. *B. alexandrina* snails have been reared in the laboratory since 2012, originating from the Theodor Bilharz Research Institute in Egypt. *B. glabrata* BS90 snails were

acquired from the Biomedical Research Institute Schistosomiasis Resource Center (Rockville, MD) and have been raised in our laboratory since 2013. All snails used in this study had a shell diameter ranging between 10-15 mm.

For each species, we sampled fourteen snails from two independent tanks over two consecutive days. These snails were then transferred to clean plastic trays (20 x 6 x 7 cm) containing approximately 500 mL water taken from their respective tanks. They were starved overnight before organ and tissue collection. To mitigate the potential impact of the sampling time, we alternated between morning and afternoon whole-snail collection and dissections for each species (Fig. 1).

2. *Biomphalaria spp.* snail sample collection.

For each individual snail, we disinfected the shell three times with 70% ethanol [15]. After cleaning the shell, we collected hemolymph through cardiac puncture using a sterile 1 mL syringe and a 22-gauge needle. The collected hemolymph was immediately placed in a sterile 1.5 mL microtube pre-cooled on ice. We then gently crushed the snail shells using sterilized glass slides and removed shell fragments using sterilized forceps. From each snail (N = 10 snails per species) (Fig. 1), we isolated the ovotestis, hepatopancreas, gut, and stomach. Once isolated, each organ was washed twice in sterile water in small sterile Petri dishes and transferred to sterile microcentrifuge tubes placed on ice. Samples were then snap-frozen in liquid nitrogen and stored at -80˚C until processing.

To analyze the microbiome of whole snails, we snap-froze four snails per species tank in liquid nitrogen. These frozen snails were individually crushed into fine powder using a pestle and mortar chilled with liquid nitrogen [16]. We transferred 100 µL aliquots of the powder to chilled microcentrifuge tubes before being stored at -80°C for gDNA extraction (Fig. 1).

Additionally, we collected two 500 µL aliquots of water from each tank where *Biomphalaria spp*. populations were raised, as well as from each tray in which the snails were housed overnight prior to dissection. These water samples were stored at -80°C and served as environmental controls.

3. DNA extraction of snail tissue.

We extracted DNA from snail organs (ovotestis, hepatopancreas, stomach, or gut), whole-snail powder, and 40 µL of hemolymph samples, as well as 40 µL of water samples from tanks or trays, was extracted using the DNeasy Blood and Tissue kit (Qiagen). The extraction procedure followed the manufacturer's protocol with the following modifications [15]. After addition of the ATL lysis buffer, we homogenized snail tissue samples (ovotestis, hepatopancreas, stomach, gut) using sterile micro-pestles. After addition of proteinase K, ovotestis, hepatopancreas, stomach, gut and whole-snail samples were incubated for 2 h in a water bath at 56°C, whilst hemolymph and water control samples were incubated for 1 h [15]. We eluted DNA in 50 µL of AE buffer for all the samples.

4. 16S rDNA V4 library construction and sequencing.

We prepared the 16S rDNA libraries in a laminar flow cabinet to avoid contamination. These were performed in triplicate to avoid potential biases introduced during PCR. We amplified ~250 bp of the 16S rDNA V4 region from bacteria and archaea, using a set of specific primers (515f and 806rB) designed by the Earth Microbiome Project [17]. The 515f forward primers were barcoded to enable sample identification. Each 16S rDNA V4 reaction consisted of 4 µL of 1x 5 Prime Hot Master Mix (QuantaBio), 2 µL of sterile PCR grade H_2O (MoBio Labs), 1 µL of 2

μM 515f barcoded primer, 1 μL of 2 μM 806rB primer (Supp. Table 1), and 2 μL of total gDNA template.

Libraries were amplified using the following thermocycler conditions: 95°C for 3 minutes, then 35 cycles of 95°C for 45 seconds, 50°C for 1 minute, 72°C for 90 seconds, then 72°C for 10 minutes. We electrophoresed 2 μL of each PCR product on agarose gel (2%) to check amplicon size, and to determine the absence of contamination in sterile water PCR controls. We pooled triplicate PCR products together (24 μL) in a 96-well plate and purified them by adding 44 μL of AMPure XP beads (Beckman Coulter). After 5-minute incubation, we placed the plates a plate magnetic device for 5 minutes. We then discarded the supernatant, and washed bead pellets twice in 200 μL of freshly-prepared 70% ethanol for 1 minute. After drying beads for 3 minutes, we removed the plate from the magnetic device, and added 20 μL of nuclease-free sterile water in each well for library elution. After a 2-minute incubation, the plate was placed on the magnetic device for 3 minutes. We then transferred each supernatant (i.e., purified 16S rDNA V4 barcoded libraries) into a fresh 96 well-plate. All incubations were done at room temperature. We quantified these libraries using the Picogreen quantification assay (Invitrogen) following the manufacturer's instructions. Finally, we made an equimass pool of all the libraries using 15 ng of each library. We quantified the final pool fragment size using the 4200 TapeStation (DNA screen tape, Agilent Technology) and molarity using the Kappa qPCR library quantification kit for the Illumina sequencing platform (following the manufacturer's recommendations). We sequenced the pool on an Illumina MiSeq sequencer (2 x 300 bp) at Texas Biomedical Research Institute (San Antonio, Texas). Raw sequencing data are accessible from the NCBI Sequence Read Archive under BioProject accession number PRJNA1113672.

5. Estimation of bacterial burden by quantitative PCR

We conducted real time quantitative PCR (qPCR) reactions to estimate the number of bacterial 16S V4 rDNA in each snail and environmental water sample. The reactions were performed in duplicate using the QuantStudio 5 (Applied Biosystems) following the protocol outlined in [15]. We normalized the 16S qPCR data for hemolymph and environmental water samples as follows:

$$q_{norm.\ 16S} = q_{16S} \times \frac{V_{elution}}{V_{sample}}$$

The bacterial density for whole-snail and organ microbiome samples may vary depending on the quantity of tissue sampled. Therefore, we normalized the 16S copy number to the number of snail cells. We estimated the number of snail cells by quantifying the single-copy gene *piwi* [18] in each sample and dividing this number by two as snails are diploid organisms. Real-time quantitative PCR for the *piwi* marker was conducted according to the methodology described in [16]. We normalized the 16S data as follows:

$$q_{norm.\ 16S} = q_{16S} \times \frac{2}{q_{piwi}}$$

6. Data processing

Commands and scripts used for processing sequencing data and performing downstream analysis are available in a Jupyter notebook on Github (https://github.com/fdchevalier/Biomphalaria-organ-microbiomes).

We demultiplexed the raw sequencing data obtained from the MiSeq using bcl2fastq (v2.17.1.14, Illumina) with the default parameters. We used the fastq files generated as input for Qiime2 (v2019.10) [19]. We checked the read quality from the results of the demux module. We then denoised and clustered the sequences into amplicon sequence variants (ASVs) using the denoise-paired command from the dada2 module with a max expected error of 5. We determined the taxonomy of the ASVs using the SILVA database (release 132) and the classify-

consensus-vsearch command of the feature-classifier module using a 97% identity threshold. ASVs with unassigned taxonomy were blasted against the NCBI nt database using megablast from blast+ (v2.9.0) to identify eukaryotic contaminants for removal in downstream analysis. We used a relatively lenient e-value threshold (1e-2) to increase our power of detection. To build a phylogenetic tree, we aligned the ASVs and masked the highly variable positions using the mafft and mask commands from the alignment module. Finally, we built and rooted a tree from the alignment using the fasttree and midpoint-root commands from the phylogeny module.

7. Statistical analysis

All statistical analyzes and graphs were performed using R software (v3.5.1). We used several packages to compute α-diversity statistics from the Qiime2 data: phyloseq [20], microbiome, and picante [21]. We compared α-diversity results using a pairwise Wilcoxon test. We used the following linear mixed-effect models to test which factor(s) influenced the α-diversity indices (1) and to test whether the collection period (morning/afternoon or day) had an impact (2):

$$\alpha\ index \sim snail\ species\ *\ sample\ type\ + (1|snail\ ID) \quad (1)$$

$$\alpha\ index \sim sample\ type\ *\ collection\ period + (1|snail\ ID) \quad (2)$$

We compared model residues with ANOVA tests from the lmerTest package [22]. Water samples were excluded from the model.

We used the vegan and the pairwiseAdonis packages to perform β-dispersion and Permanova tests, respectively. We tested for significant differences using a *t*-test or a Wilcoxon test when data did not follow a normal distribution (Shapiro test, $p < 0.05$).

We compared the microbial density between sample types using a Kruskal-Wallis test (data not following normal distribution; Shapiro test, $p < 0.05$) followed by pairwise comparison post-hoc test. We used Kendall's tau coefficient to test the correlation between the estimated

16S density in hemolymph and in organs (p-values < 0.05 were considered statistically significant).

RESULTS

1. Experimental design and library statistics

Our previous study showed that snail hemolymph harbored a diverse microbiome [15]. Here, we investigated the microbiomes associated with snail organs (gut, stomach, hepatopancreas, ovotestis) and compared these to hemolymph and whole-snail microbiomes. We sampled fourteen snails per species (*B. alexandrina* and *B. glabrata*) as outlined in Fig. 1. Snails were fasted overnight in trays filled with their respective tank water. We sampled hemolymph and organs of 10 snails and flash-froze four whole snails per species. We also sampled tank and tray water environments. We extracted DNA from each sample, and the 16S V4 rDNA region was then amplified and sequenced on a MiSeq sequencer. We obtained an average of 129,640 ± 3,782 reads per library (mean ± s.e.) (Supp. Table 2). We retained on average 50.02 ± 0.23% of the initial reads after sequencing error filtering, 49.01 ± 0.50% of the initial reads after denoising the data using the dada2 module, 43.96 ± 1.47% of the initial reads after merging reads and 42.73 ± 2.42% of the initial reads after removing chimeras. The sequencing depth was relatively even between sample types (Supp. Table 2). Rarefaction curve analysis of each library showed a plateau, indicating that our sequencing effort effectively captured the snail and environment microbiome diversity (Supp. Fig. 1).

Taxonomy assignment of the 16S rDNA sequences from all libraries revealed a total of 1,787 ASVs (amplicon sequencing variants). We excluded 29 (1.6%) ASVs assigned to

mitochondria, chloroplasts or eukaryotes. Among the remaining 1,758 ASVs, 529 ASVs (113 without taxonomic assignment) were common to *B. alexandrina* and *B. glabrata* BS90, 521 ASVs (of which 178 were without taxonomic assignment) were exclusively associated with *B. alexandrina* and 555 (of which 220 were without taxonomic assignment) were exclusively associated with *B. glabrata*.

2. Snail organs exhibit their own microbiome

a) α-diversity

We detected a microbiome in each organ investigated (stomach, gut, hepatopancreas, ovotestis) as well as in hemolymph and whole snails. The α-diversity indices (within sample type diversity) showed similar trends across both snail species (Fig. 2, Supp. Fig. 2). Hemolymph and whole snail harbored the highest number of observed ASVs, while organs exhibited approximately half of this diversity. *B. glabrata* consistently showed higher microbiome richness in organs compared to *B. alexandrina*, except for the gut which was not statistically different. This observed richness covered a diverse range of phyla, as shown by the Faith's phylogenetic diversity indices (Fig. 2). Hemolymph and whole snail displayed the most phylogenetically diverse microbiomes, whereas the organ microbiomes were the least phylogenetically diverse, except for the *B. glabrata* ovotestis. Despite this phylogenetic diversity, microbiome compositions were dominated by certain taxa, as evidenced by the Simpson evenness index (Fig. 2). The evenness of *B. alexandrina* samples (i.e. organs/hemolymph/whole snail) ranged widely, with the ovotestis displaying the most dominated microbiome, whilst the gut and hemolymph showed the least dominance. Conversely, the variation in evenness between *B. glabrata* samples was limited, with all samples being dominated by a few species.

We used a linear mixed-effects model to better understand which factors (*snail species*, *sample type* (organs/hemolymph/whole-snail) or the interaction of both) predominantly shape the α-diversity indices. For all three indices, the *sample type* was the factor with the strongest effect, followed by the interaction between *sample type* and *species*, then *species* (except for the observed richness) (Table 1). This result was mainly driven by the hemolymph and whole snails (Supp. Table 3). However, it strongly suggests that the organ and tissue environments primarily shape the microbiome diversity over the snail species. We also tested *collection time* and *day* factors using a second model, which showed no impact (Supp. Table 3).

b) β-diversity

We compared the relatedness of the organ, hemolymph and whole-snail microbiomes, as well as environmental water microbiomes, using the UniFrac index (Fig. 3). This index measures the distance between two microbiome communities using microbiome composition and microbiome phylogenetic information [23]. UniFrac index can be qualitative (presence/absence of taxa; unweighted UniFrac) or quantitative (including taxa abundance; weighted UniFrac). Differences in the unweighted UniFrac index would indicate variations in the community associated with an environment, whereas differences in the weighted UniFrac would reflect variations in the community capable of thriving in that environment.

Overall, microbiome communities tended to cluster based on organ function and physical distance between these organs, as demonstrated by both unweighted and weighted UniFrac measures in both snail species. For instance, stomach and gut microbial communities consistently clustered together, suggesting shared similarities in both composition and abundance. The hepatopancreas, which serves a liver-like function, clustered with the digestive system in unweighted UniFrac analysis, suggesting the colonization of this organ by specific taxa from the digestive system. This could be attributed to the physical intertwining of the gut

with the hepatopancreas. However, in weighted UniFrac analysis, the hepatopancreas was associated either with the digestive system (in *B. glabrata*) or the ovotestis (in *B. alexandrina*). Given the physical connection between the hepatopancreas and the ovotestis, this observation likely results from the influence of the neighboring ovotestis microbiome, with some taxa possibly colonizing the hepatopancreas. Interestingly, hemolymph and whole snail consistently clustered together in both UniFrac measures, suggesting substantial overlap between taxa found in whole snail and those in the hemolymph. However, the relative distance between hemolymph/whole-snail cluster and the organ clusters varied. In unweighted UniFrac analysis, this cluster was either farther (in *B. alexandrina*) or closer (in *B. glabrata*) from all other organs, suggesting the presence of specific, low-abundance taxa unique to this cluster. In weighted UniFrac analysis, the hemolymph/whole-snail cluster tended to be closer to the digestive system cluster, suggesting both communities share abundant taxa. Environmental samples (tray and tank waters) formed a distinct cluster, consistent with previous observations [15].

We performed PERMANOVA tests to assess the robustness of the differences observed between sample types and clusters. Firstly, we ensured that these differences were actually due to differences in group centroid distances rather than group dispersion by conducting a β-dispersion test. Groups showed similar dispersion for each comparison, except for three groups where significant differences in PERMANOVA could be due to variation in group dispersion rather than group distance (Fig. 3C). PERMANOVA tests revealed that differences in group distances were statistically significant in almost all comparisons. This finding indicates that microbiomes are specific to their respective organs, determined both by the type of taxa associated (unweighted UniFrac) and the proportion of these taxa (weighted UniFrac). While few group distances showed non-statistical differences, one consistent finding was the similarity between whole snail and hemolymph with weighted UniFrac for both snail species. This suggests that hemolymph and whole snails are dominated by similar microbial

communities and that the hemolymph microbiomes could be a reliable proxy for whole-snail microbiomes. However, some rare taxa are only found either in hemolymph or whole snail (e.g., microbes from tegument) (unweighted UniFrac). UniFrac distances between tank and tray water samples were also not significant, except with weighted UniFrac for *B. alexandrina* water. This could be due to differences in bacterial growth rates during the snail-fasting period. In *B. alexandrina*, we showed that the stomach and hepatopancreas have similar communities with the gut (unweighted UniFrac) but with a different proportion of taxa (weighted UniFrac). A similar trend was observed in *B. glabrata* between the stomach and gut microbiomes.

c) Taxonomic diversity

As observed in the beta-diversity analyses, hemolymph and organs exhibited specific taxonomic microbiome compositions but with shared similarities, either linked to organ functions (such as stomach and gut microbiomes) or localization (such as hepatopancreas and ovotestis). Additionally, hemolymph and whole-snail microbiomes showed strong similarities, suggesting once again that hemolymph could serve as a proxy for the whole-snail microbiome. These similarities were observed in both *B. alexandrina* and *B. glabrata* (Fig. 4).

Hemolymph and whole-snail samples were mainly dominated by Proteobacteria and Bacteroidetes phyla. Our previous study on hemolymph showed dominance of Bacteroidetes in *B. alexandrina* [15], which is not the case here, suggesting that hemolymph microbiome composition is dynamic. Hemolymph and whole-snail microbiomes varied mainly in the proportions of less-dominant phyla (Acidobacteria, Actinobacteria, Tenericutes, Unassigned and Verrucomicrobia). However, only Acidobacteria and Actinobacteria were consistently found in higher proportions in the hemolymph in both *B. alexandrina* and *B. glabrata*. Stomach and gut microbiomes were mainly dominated by Bacteroidetes, Proteobacteria and Tenericutes phyla. Hepatopancreas and ovotestis microbiomes were strikingly dominated by bacteria from unassigned phyla, especially in *B. alexandrina,* where these phyla comprised over 50% of the

community. These two organs may represent a very specific environment for poorly characterized bacteria. The environmental water microbiomes were dominated by Actinobacteria, Bacteroidetes, and Proteobacteria phyla. These results were similar to our previous observation [15], although Actinobacteria were found in lower proportions. Interestingly, microbiomes from tray water, in which snails were fasted overnight before sampling, showed significant variation compared to their respective tank water used as source. While conditions such as temperature, oxygenation and lighting could explain this difference, it could also imply highly dynamic water microbiomes.

3. Shared microbes between hemolymph, organs and water and between snail species

Taxonomic diversity revealed shared microbiome community patterns between sample types. Therefore, we investigated how many taxa were actually shared between these sample types (Fig. 5, Supp. Fig. 3). While sample types showed numerous distinct ASVs (especially in hemolymph and ovotestis), approximately 45% of the ASVs were shared between two or more sample types in each snail species. ASVs shared only between one snail sample type (organ or hemolymph) and whole-snail may correspond to either (i) distinct ASVs of this sample type or (ii) shared ASVs detected in this sample type and another unsampled compartment (e.g., tegument) from the whole snail.

A few trends were shared consistently between snail species. Among the shared ASVs, 40% to 50% were shared between hemolymph and ovotestis (Supp. Fig 4). Almost half (*B. alexandrina*: 45%, *B. glabrata*: 40%) of the total shared ASVs were shared between hemolymph and water samples (trays or tanks) suggesting that water serves as a source or a sink for these ASVs. Interestingly, a similar comparison between the digestive system (gut or stomach) and water samples showed that only a third of the total shared ASVs was present in both

compartments, suggesting a relatively tight control of the gut microbiome. A large proportion of shared ASVs (*B. alexandrina*: 48%, *B. glabrata*: 52%) were only found in snail samples (either whole snails or organs / hemolymph) and not in water samples, with around 12-15% of these shared ASVs found across all snail sample types. Around 7% of shared ASVs were ubiquitous, found in all snail and water sample types. Interestingly, stomach and gut microbiomes, which showed similar composition at the phyla level, shared only between 25% to 30% of ASVs (Supp. Fig 4). Hepatopancreas and ovotestis exhibited a similar trend (22% to 36%) despite being physically connected. This suggests that specific ASVs inhabit organs. Approximately 70% of ASV intersections contained 4 or less ASVs (Supp. Fig. 3). This may be due to noise or detection limits in some compartments.

We also investigated the number of ASVs of a given sample type that were shared between snail species (Fig. 6). *B. alexandrina* and *B. glabrata* shared almost half of the ASVs found in their hemolymph or water samples. However, organs of *B. glabrata* had 1.5 to 5 times more distinct ASVs than those of *B. alexandrina*. This is in-line with the greater observed richness in *B. glabrata* compared to *B. alexandrina* (Fig. 2). Whole-snail samples exhibited more shared ASVs than distinct ones. These distinct ASVs may correspond to unsampled sections of the snails, such as the tegument, which is present in whole-snail samples.

4. Snail bacterial density varies between organs

We estimated relative bacterial densities in hemolymph, organs and whole snails by quantifying the 16S rDNA copy number using qPCR (Fig. 7). Copy numbers were normalized either by volume extracted (hemolymph, water) or number of snail cells (organs and whole snails). Bacterial densities observed in the hemolymph (*B. alexandrina*: 3,227 ± 467 16S copies/µL (mean ± s.e), *B. glabrata*: 6,301 ± 1,009 16S copies/µL) were similar to those previously

quantified [15]. Four out of twenty hemolymph samples showed densities higher than 10,000 copies/µL, with one significant outlier at around 263,500 copies/µL which was excluded from the analysis. The bacterial densities observed in organs and whole snails showed consistent patterns except for the hepatopancreas. Stomach and gut microbiomes had the highest bacterial densities (*B. alexandrina*: 87.42 ± 7.31 16S copies/cell, *B. glabrata*: 136.89 ± 16.48 16S copies/cell) while the ovotestis had the lowest (*B. alexandrina*: 2.57 ± 0.30, *B. glabrata*: 0.78 ± 0.12 16S copies/cell). The bacterial densities in the hepatopancreas showed intermediate levels and strong differences between snail species. For instance, *B. alexandrina* showed a broader dispersion compared to *B. glabrata*, with 68.84 ± 6.42 and 19.05 ± 3.75 16S copies/cells in the hepatopancreas, respectively. These differences could be biological or artefactual due to gut remnants remaining intertwined within the hepatopancreas. Whole snails showed a limited number of 16S copies per cell with a similar pattern between both species (*B. alexandrina*: 2.12 ± 0.77, *B. glabrata*: 4.21 ± 1.07 16S copies/cell).). This apparent overall low bacterial density is likely due to the head-foot of the snail, which constitutes a high proportion of the whole-snail sample but likely have low bacterial content.

We also investigated whether bacterial densities were linked between sample types, particularly whether a higher hemolymph density would be associated with higher organ densities. We did not find consistent correlations between organs or any correlation between hemolymph and organs (Supp. Table 3). This suggests that bacterial densities appear to be independently regulated in adjacent organ compartments or hemolymph.

DISCUSSION

1. Snail organs and hemolymph have diverse and distinct microbiomes

Our analyses confirmed the presence of microbiomes associated with stomach, gut, hepatopancreas and ovotestis organs. These organ microbiomes clustered separately from the hemolymph microbiome and had lower α-diversity scores. Microbial α-diversity was primarily driven by the sample type (organs, hemolymph or whole-snail) rather than the snail species, suggesting organ habitat strongly influences α-diversity. In addition, microbiomes tended to cluster by organ functions, suggesting microbiome specializations. This pattern is also observed when comparing transcriptomes from different tissues in mammals: gene expression clustered primarily by organs rather than species [24]. This may reveal interesting parallels between transcriptomic and microbiome fields, where units (expressed genes, microbes) could generate metabolic networks that define organ functions.

These specific organ and tissue microbiomes highlight the importance of investigating microbiomes at the organ level rather than the whole-organism level to obtain a more precise and robust picture. While the investigation of organ microbiomes is apparent in vertebrates due to their size, this approach has received limited attention in small invertebrates. A few studies have explored organ microbiomes in mollusks (oysters, mussels [7–9]) and crustaceans (terrestrial crabs [10] and isopods [11]). Interestingly, for some, but not all, of these organisms there were similar microbial patterns to those observed in snails. For instance, hemolymph and gut microbiomes tend to cluster by sample types rather than species in oysters (*Crassostrea gigas*) and Mediterranean mussels (*Mytilus galloprovincialis*) [7]. Additionally, the hemolymph microbiome showed higher observed richness than the gut, and this organ exhibited a similar richness to that of the surrounding water, as observed in our snails. Another analysis of the Mediterranean mussel showed specific microbiomes for the hemolymph, gill, stomach, gut and

foot, which were all different from the water environment [8]. However, α-diversity in the hemolymph was similar to that in the gut in this study. In crustaceans, the terrestrial brachuryan crab *Chiromantes haematocheir* showed specific organ microbiomes (in several gut sections, gills, and gonads) with very limited α-diversity compared to the environment [10]. Similar to our finding, the organ microbiomes from different crab populations clustered by organ rather than by host population. The terrestrial isopod *Armadillidium vulgare* also showed limited microbiome α-diversities in organs (nerve cord, digestive systems, gonads, and hemolymph) compared to environment samples. However, their microbiomes clustered by population (field or laboratory) rather than by organs. While some of these differences may be attributed to technical factors (sample processing or analysis pipeline), they may also highlight species specificities in managing organ microbiomes which requires further investigation.

Snail microbiome studies have mainly focused on the gut (see [25] for review). This organ is of importance because its microbiome is involved in nutrient acquisition, which may have significant impact on host and parasite fitness, and may ultimately influence species evolution [26]. We found that the snail stomach and gut have the highest densities of bacteria per host cells, while exhibiting the least α-diverse microbiomes. The dramatic difference in microbiome diversity (α and β) between the digestive system and the hemolymph provides an ideal opportunity to better understand how microbiomes respond to pathogens. Snails could serve as an excellent model, given their susceptibility to a wide array of pathogens and parasites [27]. Additionally, pathogens can be found in different tissues of snails. For instance, *Angiostrongylus* nematodes develop in the gut, while *Schistosome* trematodes develop into the hepatopancreas and ovotestis, which are bathed by the hemolymph. Variations in organ microbiome and pathogen diversity opens the way to investigate microbiome perturbation and adaptation both at site of infection (local) and at a systemic scale (distal).

2. Whole snail: the importance of the shell

The whole-snail microbiome is another major area of study and was used for the first characterization of the *Biomphalaria* microbiome [28]. This approach is still in use today [29–35]. While sequencing a single “whole microbiome” per sample is cost efficient and can provide a snapshot of the diversity within the entire organism, it may also mask specific microbiome dynamics. In our study design, we included the analyses of whole-snail microbiomes to investigate how representative they were compared to organ microbiomes. Whole-snail microbiomes exhibited one of the highest levels of α-diversity, comparable to that of hemolymph microbiome. Interestingly, these whole-snail microbiomes were also similar in composition to hemolymph microbiomes, rather than reflecting a composite of the organ and hemolymph microbiomes. Hemolymph therefore, could serve as proxy for investigating whole-snail microbiome diversity, potentially enabling longitudinal studies of individual snail microbiomes through regular bleeding.

While studying whole-snail microbiomes can address specific questions, the results might be influenced by sample preparation methodology. The two identified strategies for preparing whole-snail samples involve either keeping the snail shell intact or removing it before homogenizing snail bodies. This may significantly impact microbiome results and makes direct comparisons between studies challenging. Shell removal is usually done by peeling the shell [28,30–32]. This strategy offers three advantages: (i) it reduces potential contamination from the shell, (ii) facilitates sample homogenization, which can be challenging with hard shells, and (iii) can limit PCR reaction inhibition by reducing the carryover of inhibitors such as calcium ions. However, shell peeling is likely to result in snail bleeding due to snail body retraction or tegumental damage. In the present study, we demonstrated that the hemolymph microbiome exhibits the highest α-diversity, and that the microbiome from whole snails (prepared with the

shell intact) showed similar α-diversity to the hemolymph microbiome. Furthermore, the whole-snail microbiome had greater similarity to hemolymph microbiome than to organ microbiomes (β-diversity), and a significant number of ASVs were shared between the whole-snail and hemolymph microbiomes. Hemolymph bleeding during shell removal could result in significant loss of bacteria, potentially limiting the capture of the entire diversity of the whole-snail microbiome. Therefore, to understand the consequences of sample preparation on the accuracy of microbiome diversity (α, β and taxonomic) estimation, comparing of whole-snail microbiomes prepared with and without the shell is necessary.

3. Hemolymph and ovotestis: hotspots of microbial diversity?

Hemolymph and ovotestis harbored the highest number of total ASVs and the highest number of distinct ASVs compared to the other snail organs (Fig. 5). This finding is surprising considering that the hemolymph contains immune cells whose roles are to target and kill microbes. While the role of the hemolymph microbiome, if any, remains unknown, the maintenance of a diverse microbiome through tolerance mechanisms may serve to control microbial populations by promoting competition between microbes and limiting immune reactions to prevent host damage, as observed in the gut of vertebrates [36]. The presence of a diverse microbiome in the ovotestis is also surprising because it is the most remote organ in the snail's anatomy, located at the center of the coiled shell. This positioning should limit its contact with the hemolymph and other organs, and their respective microbiomes. This remote position of the ovotestis could explain why it has the lowest bacterial density of all organs. This low bacterial density coupled with the high diversity is likely responsible for the variable clustering position of the ovotestis microbiome relative to the other organ microbiomes (Fig. 3), either clustering with the neighboring hepatopancreas (*B. alexandrina*), or clustering separately

from any organs (*B. glabrata*). While the role of the ovotestis microbiome remains to be defined, we hypothesize that the diverse range of bacteria may provide nutrients and metabolites required for egg production. Understanding the reason behind this diversity could be crucial for developing future strategies based on disrupting organ microbiomes to control snail populations.

Ovotestis microbiomes were characterized by a high proportion of unassigned taxa. This trait is shared with the hepatopancreas and, to a lesser extent, with the hemolymph. The proportion of unassigned taxa was higher in *B. alexandrina* compared to *B. glabrata*. Characterizing these bacteria will be critical for better understanding their potential contribution to ovotestis physiology.

4. Implications of organ specific microbiomes

Snails are vectors of a variety of trematode parasites [27]. During several weeks of host infection, parasites develop through different stages, migrating through snail tissues and developing within snail organs. We previously hypothesized that parasites are exposed to the hemolymph microbiome [15]. However, our present study shows that they are exposed to an even more diverse range of microbiomes within snail organs. This raises three main questions: (i) How do these host microbiomes respond to the presence of parasites, and are there any tissue/organ specific reactions? (ii) How do host microbiomes influence parasites and their life-history traits (e.g. compatibility, development time, production of cercariae, etc.)? (iii) Do parasites acquire host microbiomes? To date, only a limited number of studies have investigated the impact of parasite infection on snail microbiome [32,35,37]. However, these studies primarily focused on whole-snail microbiomes or feces. The latter approach may be limiting due to the masking effect of the entire snail microbiome on specific changes in organ or hemolymph microbiomes.

In addition of bacteria and archaea, the presence of microeukaryotes in *B. glabrata* has recently been investigated [33]. In this study, authors showed co-variation of microeukaryotes and bacteria with planorbid species. While this is a significant step forward as this group of microorganisms is often overlooked, the observed co-variation was at the whole-snail level. These microeukaryotes could potentially exhibit similar organ-specific distributions as seen with the bacteria. Investigating this distribution may provide future insights into this co-variation and reveal subtler patterns that have not yet been identified.

The presence of microbiomes associated with organs raises questions about localization and colonization. While we can expect the microbes of the digestive system to be mainly localized in the lumen of the organs and those of the hemolymph to be free-floating, the localization of microbes in the hepatopancreas and ovotestis is still to be determined. While insects have specialized structure (bacteriocytes) to harbor symbiotic microorganisms [38], it is unknown whether snail microbes are localized randomly on the surface of the organ or tend to occupy specific areas within the organs, such as ducts or other dedicated structures. Additionally, the mode of microbial colonization of the organ is another area to investigate. We showed some microbes are ubiquitous in the snails and not detected in the environment. This suggests wide dispersion of the microbes within the snails, possibly through connection between organs or leakage. Tracking labelled microbes could be used to investigate the paths used to colonize their host [39].

While some microbes are ubiquitously found across all organs and hemolymph, the majority of remaining microbes are distinct to each compartment. This suggests that microbiome homeostasis is maintained within each organ and hemolymph. This maintenance might be passive, with specialized microbes thriving in these different environments, or more active, with specific mechanisms used by the snail to select them. Potential co-adaptation between snails and their microbiomes could be genetically mediated, as a snail genetic locus

has been associated with specific microbe abundance using whole-snail microbiome analysis [30]. Performing similar association studies at the organ or hemolymph level could be more powerful for detecting genetic determinants controlling host-microbe associations.

Distances between whole-snail microbiome communities of different snail species have been found to be correlated with genetic distances between snail species, suggesting phylosymbiosis [31]. Phylosymbiosis has been demonstrated in both invertebrates and vertebrates [40], and can occur between different sections of the same organ in vertebrates (e.g. along the length of the gastrointestinal tract in rodents [41]). It is likely that similar observations could be made in invertebrates. The presence of diverse and organ-specific microbiomes in snails could provide an excellent model for investigating the existence of phylosymbiosis at the organ level in invertebrates.

5. Limitations

Our characterization of snail organ microbiomes revealed diverse and specific organ microbiomes. However, some of our results may be influenced by aspects of our study design. Firstly, we did not control for snail age in both species, which may explain some of the observed variation in microbiomes. We sampled snails of similar sizes but, while size is correlated with age, it is also influenced by population density [42]. Since the dynamics of snail microbiomes during aging are unknown, it is possible that some of the differences observed between or within species are due to snail age and physiological state. For example, the greater variation in bacterial density observed in the hepatopancreas of *B. glabrata* could be attributed to physiological differences, such as gut leakage.

Secondly, we sampled snail microbiomes at a single timepoint which prevented us from testing the stability of microbiome differences in the long term. However, we think that our

results should be robust to short-term variations, as we integrated morning and afternoon sampling to limit possible effects of daily chronobiological variations, and we sampled two independent tanks to minimize batch effects.

Finally, all snails from the two species studied here were raised in a similar environment (i.e., exposed to the same water and food sources). This similarity in environmental conditions may partially explain why the organ, rather than the species, is the main factor responsible for microbiome differences. To confirm the preeminence of the organ factor in shaping snail microbiome diversity, we plan to analyze organ microbiomes from different snail species co-existing in various settings or natural locations, similar to the approach used for bivalve mollusks [7] and crabs [10].

DECLARATIONS:

Ethics approval and consent to participate:

Not applicable

Consent for publication:

Not applicable

Funding:

This research was supported by the Texas Biomed Internship program (LVC), the Burroughs Wellcome Fund (LVC), University of Glasgow (IBAHCM_stipend_144536 (LVC)), NIH grants (NIH R01AI133749 and R01AI123434 (TJCA); NIH R21AI171601 (FC/WL)), and was conducted in facilities constructed with support from Research Facilities Improvement Program grant C06 RR013556 from the National Center for Research Resources.

Availability of data and materials:

Raw sequencing data are accessible from the NCBI Sequence Read Archive under BioProject accession number PRJNA1113672. Commands and scripts used for processing sequencing data and performing downstream analysis are available in a Jupyter notebook on Github (https://github.com/fdchevalier/Biomphalaria-organ-microbiomes).

Competing interests:

The authors declare that they have no competing interests.

Authors' contributions:

LVC, TJCA, FDC, and WL designed the experiments. LVC prepared and collected the samples, extracted DNA and prepared the 16S libraries and sequencing run. SCN performed the qPCR assays. LVC and FDC performed all the data analyses. LVC, FDC and WL wrote the first version of the manuscript. All authors edited the manuscript and approved the final version.

Acknowledgements:

We thank the Biomedical Research Institute (NIAID Schistosomiasis Resource Center, Rockville, MD) for providing the BgBS90 snails through NIH-NIAID Contract HHSN272201700014I, and the Theodor Bilharz Research Institute (Giza, Egypt) for providing *B. alexandrina* snails. We thank Dr. Shelley Cole and Vanessa Ayala (Texas Biomedical Research Institute) for their help with MiSeq sequencing.

REFERENCES

1. Colston TJ, Jackson CR. Microbiome evolution along divergent branches of the vertebrate tree of life: what is known and unknown. Molecular Ecology. 2016;25:3776–800.

2. Petersen JM, Osvatic J. Microbiomes in natura : Importance of invertebrates in understanding the natural variety of animal-microbe interactions. mSystems. 2018;3.

3. Ogunrinola GA, Oyewale JO, Oshamika OO, Olasehinde GI. The human microbiome and its impacts on health. International journal of microbiology. 2020;2020:8045646.

4. Kolodny O, Callahan BJ, Douglas AE. The role of the microbiome in host evolution. Philosophical Transactions of the Royal Society B: Biological Sciences. 2020;375:20190588.

5. Aldridge S, Teichmann SA. Single cell transcriptomics comes of age. Nature communications. 2020;11:4307.

6. Li X, Wang C-Y. From bulk, single-cell to spatial RNA sequencing. International journal of oral science. 2021;13:36.

7. Vezzulli L, Stagnaro L, Grande C, Tassistro G, Canesi L, Pruzzo C. Comparative 16SrDNA gene-based microbiota profiles of the pacific oyster (*Crassostrea gigas*) and the mediterranean mussel (*Mytilus galloprovincialis*) from a shellfish farm (ligurian sea, italy). Microbial ecology. 2018;75:495–504.

8. Musella M, Wathsala R, Tavella T, Rampelli S, Barone M, Palladino G, et al. Tissue-scale microbiota of the Mediterranean mussel (Mytilus galloprovincialis) and its relationship with the environment. The Science of the total environment. 2020;717:137209.

9. Leite L, Jude-Lemeilleur F, Raymond N, Henriques I, Garabetian F, Alves A. Phylogenetic diversity and functional characterization of the Manila clam microbiota: a culture-based approach. Environmental science and pollution research international. 2017;24:21721–32.

10. Bacci G, Fratini S, Meriggi N, Cheng CLY, Ng KH, Pindo M, et al. Conserved organ-specific microbial assemblages in different populations of a terrestrial crab. Frontiers in Microbiology. 2023;14.

11. Dittmer J, Lesobre J, Moumen B, Bouchon D. Host origin and tissue microhabitat shaping the microbiota of the terrestrial isopod *Armadillidium vulgare*. FEMS microbiology ecology. 2016;92:fiw063.

12. World Health Organization. Schistosomiasis [Internet]. 2023. Available from: https://www.who.int/news-room/fact-sheets/detail/schistosomiasis

13. James SL, Abate D, Abate KH, Abay SM, Abbafati C, Abbasi N, et al. Global, regional, and national incidence, prevalence, and years lived with disability for 354 diseases and injuries for 195 countries and territories, 1990–2017: a systematic analysis for the Global Burden of Disease Study 2017. The Lancet. 2018;392:1789–858.

14. Verjee MA. Schistosomiasis: Still a cause of significant morbidity and mortality. Research and Reports in Tropical Medicine. 2020;Volume 10:153–63.

15. Chevalier FD, Diaz R, McDew-White M, Anderson TJC, Le Clec'h W. The hemolymph of *Biomphalaria* snail vectors of schistosomiasis supports a diverse microbiome. Environmental microbiology. 2020;22:5450–66.

16. Le Clec'h W, Diaz R, Chevalier FD, McDew-White M, Anderson TJC. Striking differences in virulence, transmission and sporocyst growth dynamics between two schistosome populations. Parasites & Vectors. 2019;12.

17. Apprill A, McNally S, Parsons R, Weber L. Minor revision to V4 region SSU rRNA 806R gene primer greatly increases detection of SAR11 bacterioplankton. Aquat Microb Ecol. 2015;75:129–37.

18. Odoemelam E, Raghavan N, Miller A, Bridger JM, Knight M. Revised karyotyping and gene mapping of the *Biomphalaria glabrata* embryonic (Bge) cell line. Int J Parasitol. 2009;39:675–81.

19. Bolyen E, Rideout JR, Dillon MR, Bokulich NA, Abnet CC, Al-Ghalith GA, et al. Reproducible, interactive, scalable and extensible microbiome data science using QIIME 2. Nature biotechnology. 2019;37:852–7.

20. McMurdie PJ, Holmes S. phyloseq: an R package for reproducible interactive analysis and graphics of microbiome census data. PloS one. 2013;8:e61217.

21. Kembel SW, Cowan PD, Helmus MR, Cornwell WK, Morlon H, Ackerly DD, et al. Picante: R tools for integrating phylogenies and ecology. Bioinformatics (Oxford, England). 2010;26:1463–4.

22. Kuznetsova A, Brockhoff PB, Christensen RHB. lmerTest Package: Tests in linear mixed effects models. Journal of Statistical Software. 2017;82:1–26.

23. Lozupone CA, Hamady M, Kelley ST, Knight R. Quantitative and qualitative beta diversity measures lead to different insights into factors that structure microbial communities. Applied and environmental microbiology. 2007;73:1576–85.

24. Gilad Y, Mizrahi-Man O. A reanalysis of mouse ENCODE comparative gene expression data. F1000Research. 2015;4:121.

25. Li P, Hong J, Yuan Z, Huang Y, Wu M, Ding T, et al. Gut microbiota in parasite-transmitting gastropods. Infectious Diseases of Poverty. 2023;12.

26. Moeller AH, Sanders JG. Roles of the gut microbiota in the adaptive evolution of mammalian species. Philosophical transactions of the Royal Society of London Series B, Biological sciences. 2020;375:20190597.

27. Pathak CR, Luitel H, Utaaker KS, Khanal P. One-health approach on the future application of snails: a focus on snail-transmitted parasitic diseases. Parasitology research. 2023;123:28.

28. Ducklow HW, Boyle PJ, Maugel PW, Strong C, Mitchell R. Bacterial flora of the schistosome vector snail *Biomphalaria glabrata*. Appl Environ Microbiol. 1979;38:667–72.

29. Silva TM, Melo ES, Lopes ACS, Veras DL, Duarte CR, Alves LC, et al. Characterization of the bacterial microbiota of *Biomphalaria glabrata* (Say, 1818) (Mollusca: Gastropoda) from Brazil. Letters in applied microbiology. 2013;57:19–25.

30. Allan ERO, Tennessen JA, Sharpton TJ, Blouin MS. Allelic variation in a single genomic region alters the microbiome of the snail *Biomphalaria glabrata*. The Journal of heredity. 2018;109:604–9.

31. Huot C, Clerissi C, Gourbal B, Galinier R, Duval D, Toulza E. Schistosomiasis vector snails and their microbiota display a phylosymbiosis pattern. Frontiers in microbiology. 2020;10:3092.

32. Portet A, Toulza E, Lokmer A, Huot C, Duval D, Galinier R, et al. Experimental infection of the *Biomphalaria glabrata* vector snail by *Schistosoma mansoni* parasites drives snail microbiota dysbiosis. Microorganisms. 2021;9.

33. Clerissi C, Huot C, Portet A, Gourbal B, Toulza E. Covariation between microeukaryotes and bacteria associated with Planorbidae snails. PeerJ. 2023;11:e16639.

34. Schols R, Vanoverberghe I, Huyse T, Decaestecker E. Host-bacteriome transplants of the schistosome snail host Biomphalaria glabrata reflect species-specific associations. FEMS microbiology ecology. 2023;99.

35. McCann P, McFarland C, Megaw J, Siu-Ting K, Cantacessi C, Rinaldi G, et al. Assessing the microbiota of the snail intermediate host of trematodes, Galba truncatula. Parasites & vectors. 2024;17:31.

36. Swiatczak B, Cohen IR. Gut feelings of safety: tolerance to the microbiota mediated by innate immune receptors. Microbiology and immunology. 2015;59:573–85.

37. Osório JB, de Mattos Pereira L, Giongo A, Marconatto L, Potriquet J, Candido RRF, et al. Mollusk microbiota shift during Angiostrongylus cantonensis infection in the freshwater snail Biomphalaria glabrata and the terrestrial slug Phillocaulis soleiformis. Parasitology research. 2020;119:2495–503.

38. Chomicki G, Werner GDA, West SA, Kiers ET. Compartmentalization drives the evolution of symbiotic cooperation. Philosophical transactions of the Royal Society of London Series B, Biological sciences. 2020;375:20190602.

39. Geva-Zatorsky N, Alvarez D, Hudak JE, Reading NC, Erturk-Hasdemir D, Dasgupta S, et al. In vivo imaging and tracking of host-microbiota interactions via metabolic labeling of gut anaerobic bacteria. Nature medicine. 2015;21:1091–100.

40. Brooks AW, Kohl KD, Brucker RM, van Opstal EJ, Bordenstein SR. Phylosymbiosis: Relationships and functional effects of microbial communities across host evolutionary history. PLoS biology. 2016;14:e2000225.

41. Kohl KD, Dearing MD, Bordenstein SR. Microbial communities exhibit host species distinguishability and phylosymbiosis along the length of the gastrointestinal tract. Molecular ecology. 2018;27:1874–83.

42. Mangal TD, Paterson S, Fenton A. Effects of snail density on growth, reproduction and survival of *Biomphalaria alexandrina* exposed to *Schistosoma mansoni*. Journal of parasitology research. 2010;2010.

TABLES

Table 1 – ANOVA results of the linear mixed effect model on factors shaping microbiome diversity. We explored the impact of snail species and samples types (organs, hemolymph and whole snails) on three α-diversity indices. The most significant factor shaping the diversity is the sample type followed by the interaction between species and sample type and finally the species for Faith's phylogenetic diversity and Simpson evenness.

		Observed richness		Faith's Phylogenetic diversity		Simpson evenness	
	Degrees of freedom	F value	p-value	F value	p-value	F value	p-value
Species	1	0.3945	0.5306	7.0782	0.008515	6.9125	0.009378
Sample type	5	34.0345	3.331e-12	55.9449	6.132e-15	18.8117	1.219e-08
Species:Sample type	5	15.9995	6.840e-09	21.6285	8.048e-11	8.3467	7.275e-06

FIGURES

Fig. 1 – Experimental design. We sampled 14 *Biomphalaria alexandrina* (Ba) and 14 *B. glabrata* (BgBS90) snails from two different tanks alternately in the morning or the afternoon. We fasted the snails overnight in trays containing water from their respective tanks. For each batch, we sampled hemolymph, then stomach, gut, hepatopancreas (liver) and ovotestis from five snails, and snap-froze two whole snails. We sampled tank and tray waters as environmental controls. We extracted DNA from each sample to prepare 16S rDNA libraries, and sequenced these libraries on a MiSeq platform.

Fig. 2 – α-diversity indices of snail hemolymph, organs, whole snails, and water. We computed three α-diversity indices: observed ASVs (raw number of ASVs), Faith's phylogenetic Diversity (based on phylogenetic distance between ASVs), and Simpson evenness (true evenness of taxa within a sample independently of taxa richness; a value of 0 means uneven taxa distribution in a sample). The highest diversity is found in hemolymph and whole snail samples. The two snail species (*B. alexandrina* (Ba) and *B. glabrata* (BgBS90)) showed differences in their diversity, especially between organs. All these bacterial communities are dominated by characteristic bacterial species. Hm: hemolymph, S: stomach, G: gut, Hp: hepatopancreas, O: ovotestis, W: whole snail, Ty: tray water, Tk: tank water. Each box plot represents the median and the interquartile ranges of the distribution. Statistical test is available in Supp. Table 3.

Fig. 3 – β-diversity indices of snail hemolymph, organs, whole snails, and water. We computed UniFrac indices: unweighted and weighted UniFrac. UniFrac measures account for the phylogenetic distance of the microbial taxa when measuring distances between groups. These measures can be weighted by the abundance of each microbial taxa. The matrices on

the right side of each index showed the significance level of the Permanova test (differences between sample types) and the β dispersion test (homogeneity of variance between sample types confirming that significant PERMANOVA results are due to differences in distance between groups and not to differences in sample dispersion between groups). Organ microbiomes tend to cluster by functions. Whole-snail microbiomes are similar to hemolymph microbiomes. Ba: *B. alexandrina*, BgBS90: *B. glabrata*; Hm: hemolymph, S: stomach, G: gut, Hp: hepatopancreas, O: ovotestis, W: whole snail, Ty: tray water, Tk: tank water.

Fig. 4 – Taxonomic diversity of sample types in each snail species. Relative abundance of the different phyla in each sample type for each snail species (A & B). Composition varies between sample types with Bacteroidetes, Proteobacteria, Tenericutes and unassigned phyla dominating snail sample types, and with Actinobacteria and Proteobacteria phyla dominating water samples. Composition is more similar between organs sharing functions (stomach and gut) or location (hepatopancreas and ovotestis). Proportion of unassigned phyla is high in snail sample types, particularly in *B. alexandrina* hepatopancreas and ovotestis. Ba: *B. alexandrina*, BgBS90: *B. glabrata*; Hm: hemolymph, S: stomach, G: gut, Hp: hepatopancreas, O: ovotestis, W: whole snail, Ty: tray water, Tk: tank water.

Fig. 5 – Shared ASVs between sample types by species. These upset plots show the number of ASVs (left horizontal barplot) and the number of ASV (upright barplot) for each intersection (dot plot) for *B. alexandrina* (Ba) and *B. glabrata* (BgBS90). For readability, we removed intersections with less than five ASVs. The full intersection set is available in Supp. Fig. 3. A significant proportion of ASVs are distinct, mainly found in the hemolymph and ovotestis. Some ASVs are also found ubiquitously in the snails but not in the environment. Hm:

hemolymph, S: stomach, G: gut, Hp: hepatopancreas, O: ovotestis, W: whole snail, Ty: tray water, Tk: tank water.

Fig. 6 – Shared ASVs between species by sample types. Barplots showed the number of distinct ASVs by species or shared between species for each sample type. Shared ASV between the two species are usually representing between a third to half of the ASV of a given sample type. *B. glabrata* (BgBS90) tends to have more distinct ASVs than *B. alexandrina* (Ba).

Fig. 7 – Comparison of 16S density between snail organs, whole snail, hemolymph and water. We quantified raw 16S copy number either host cell (organ and whole snail) or per microliter of hemolymph and water using qPCR. Stomach and gut had the highest densities, ovotestis the lowest, with species-specific variations in hepatopancreas densities. Hemolymph densities were consistent with previous studies. S: stomach, G: gut, Hp: hepatopancreas, O: ovotestis, W: whole snail, Hm: hemolymph, Ty: tray water, Tk: tank water.

SUPPLEMENTARY FILES

Supp. Fig. 1 – Rarefaction curves. Curves were plotted for each sample type (Hm: hemolymph, S: stomach, G: gut, Hp: hepatopancreas, O: ovotestis, W: whole snail, Ty: tray water, Tk: tank water). Each of these curves plateau demonstrating that sampling more reads (x axis) would not have increased ASVs richness (y axis).

Supp. Fig. 2 – α-diversity statistical results. We performed Wilcoxon pairwise comparisons between the different sample types of *B. alexandrina* (Ba) and *B. glabrata* (BgBS90) for each α-diversity index (Fig. 2). The p-values are not adjusted for multiple comparisons. Results in these comparisons are similar to the linear mixed-effect model results (Supp. Table 3).

Supp. Fig. 3 – Shared ASVs between sample types by species (full set).

Supp. Fig. 4 – Proportion of shared ASVs between sample types in pairwise comparisons. The upper and lower triangles correspond to sample types of *B. alexandrina* (Ba) and *B. glabrata* (BgBS90), respectively.

Supp. Fig. 5 – 16S density statistical results. We performed Wilcoxon pairwise comparisons between the organs/whole snails or hemolymph/water of *B. alexandrina* (Ba) and *B. glabrata* (BgBS90) for the 16S density (Fig. 7). The p-values are not adjusted for multiple comparisons. S: stomach, G: gut, Hp: hepatopancreas, O: ovotestis, W: whole snail, Hm: hemolymph, Ty: tray water, Tk: tank water.

Supp. Table 1 – Earth Microbiome Project primers used for generating each library.

Supp. Table 2 – Library statistics.

Supp. Table 3 – Linear mixed-effect model results.

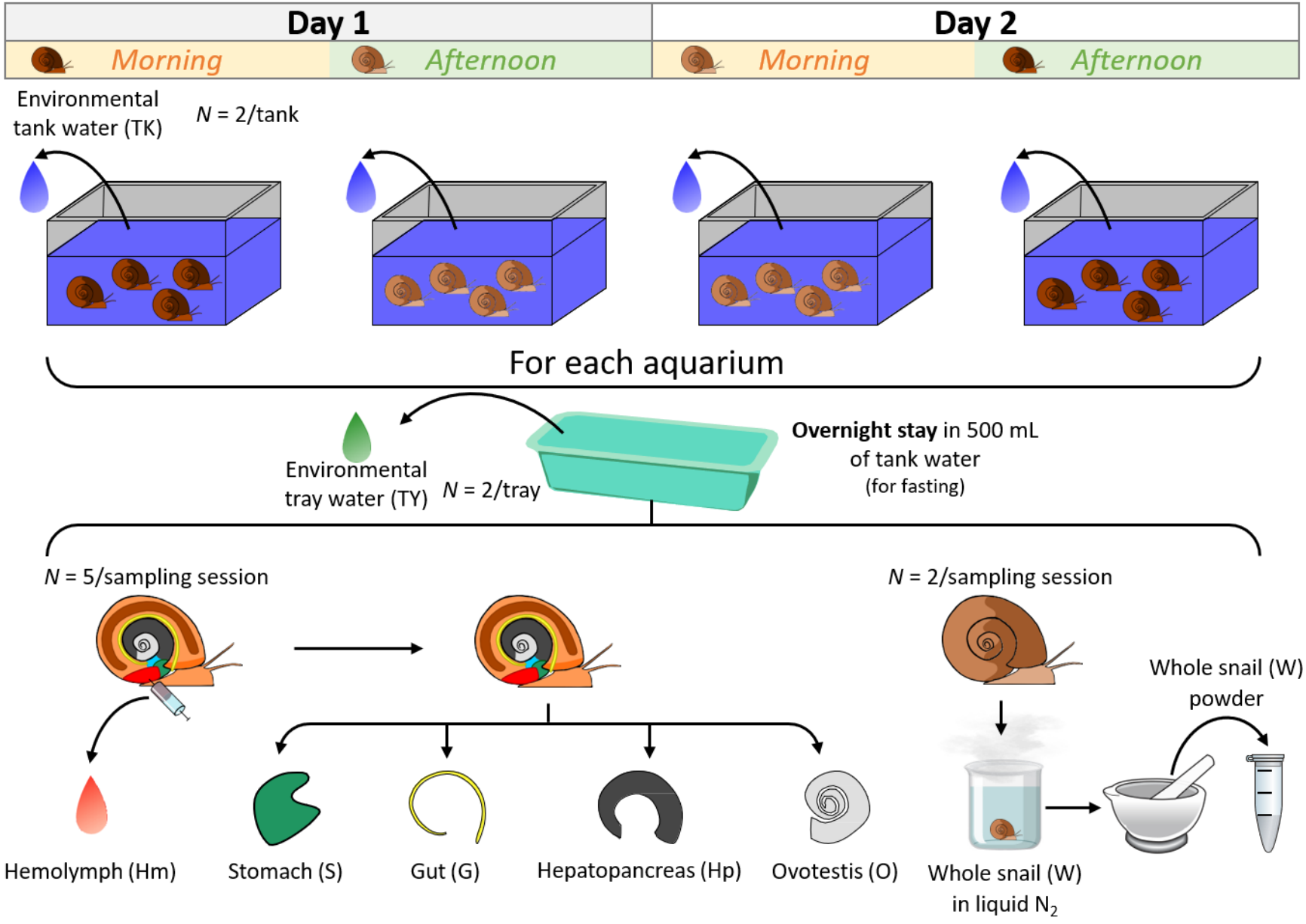
Day 1
Day 2
Morning
Afternoon
Morning
Afternoon
Environmental tank water (TK)
N = 2/tank
For each aquarium
Environmental tray water (TY)
N = 2/tray
Overnight stay in 500 mL of tank water (for fasting)
N = 5/sampling session
N = 2/sampling session
Whole snail (W) powder
Hemolymph (Hm)
Stomach (S)
Gut (G)
Hepatopancreas (Hp)
Ovotestis (O)
Whole snail (W) in liquid N2

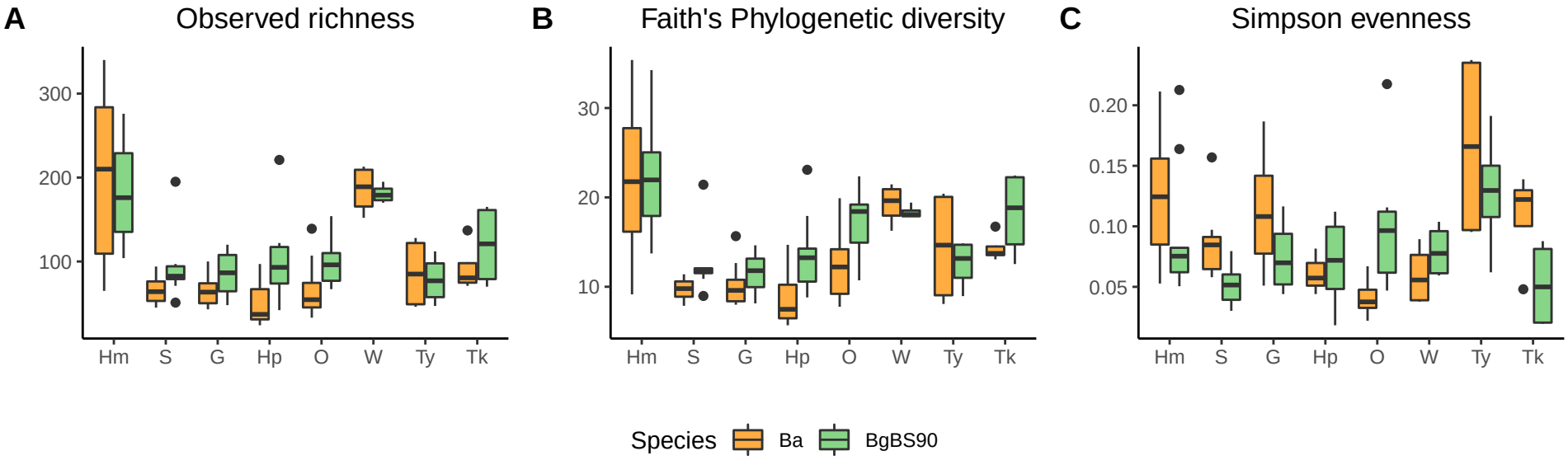
A
Observed richness
300
200
100
Hm
S
G
Hp
O
W
Ty
Tk
B
Faith's Phylogenetic diversity
30
20
10
Hm
S
G
Hp
O
W
Ty
Tk
C
Simpson evenness
0.20
0.15
0.10
0.05
Hm
S
G
Hp
O
W
Ty
Tk
Species
Ba
BgBS90

A. Ba − Unweighted UniFrac

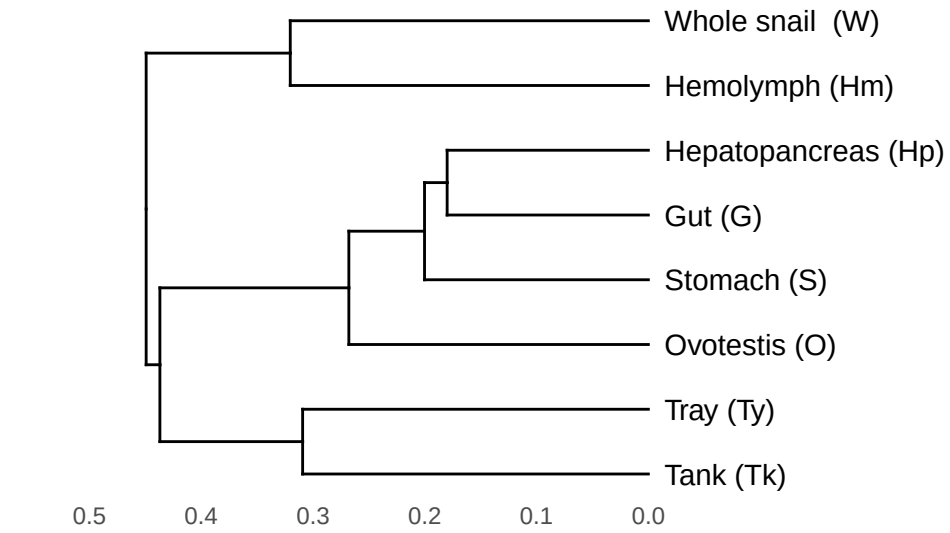

Permanova test \ β−dispersion test	Hm	S	G	Hp	O	W	Ty	Tk
Tk	1.2e−02	4.3e−03	2.5e−03	2.5e−03	8.7e−03	4.5e−02	2.6e−01	
Ty	1.2e−02	2.5e−03	6.0e−03	2.5e−03	1.4e−02	3.0e−02		9.8e−01
W	3.3e−02	2.5e−03	2.5e−03	2.5e−03	4.3e−03		1.0e+00	1.0e+00
O	1.5e−02	2.5e−03	1.8e−02	8.7e−03		9.8e−01	8.3e−01	1.0e+00
Hp	2.5e−03	9.9e−03	2.3e−01		1.0e+00	1.0e+00	9.5e−01	1.0e+00
G	2.5e−03	6.8e−02		1.0e+00	1.0e+00	1.0e+00	9.6e−01	1.0e+00
S	2.5e−03		1.0e+00	1.0e+00	9.6e−01	1.0e+00	1.0e+00	1.0e+00
Hm		9.8e−01	1.0e+00	1.0e+00	1.0e+00	9.9e−01	8.9e−01	1.0e+00

B. Ba − Weighted UniFrac

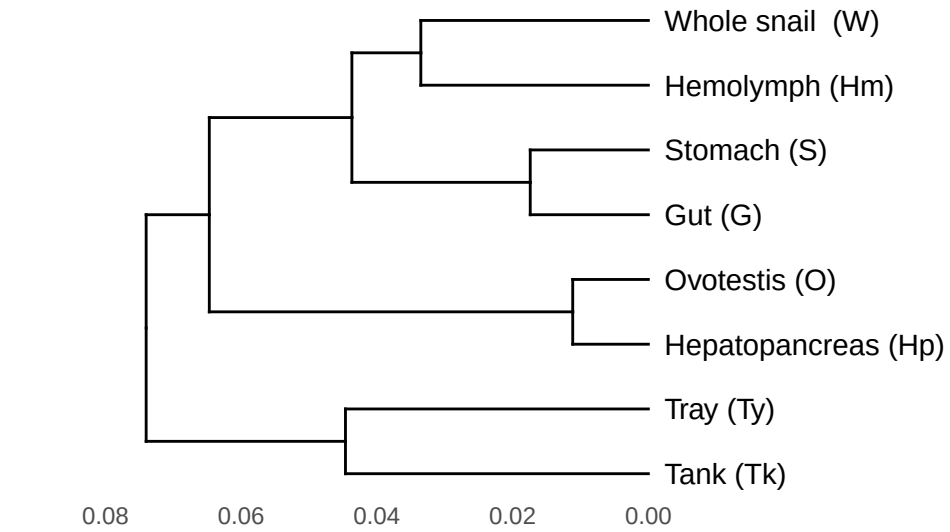

Permanova test \ β−dispersion test	Hm	S	G	Hp	O	W	Ty	Tk
Tk	5.9e−03	2.8e−03	3.3e−03	3.3e−03	2.8e−03	4.5e−02	4.1e−02	
Ty	3.3e−03	2.8e−03	3.3e−03	2.8e−03	2.8e−03	3.0e−02		1.0e+00
W	1.3e−01	5.9e−03	8.0e−03	3.3e−03	2.8e−03		1.0e+00	1.0e+00
O	3.3e−03	2.8e−03	2.8e−03	6.4e−01		9.5e−01	1.0e+00	9.7e−01
Hp	2.8e−03	2.8e−03	3.3e−03		1.0e+00	9.8e−01	1.0e+00	9.9e−01
G	7.0e−03	4.7e−02		4.3e−01	3.3e−01	1.0e+00	9.3e−01	1.0e+00
S	1.1e−02		1.0e+00	2.8e−01	2.1e−01	9.9e−01	8.6e−01	9.8e−01
Hm		9.9e−01	1.0e+00	7.7e−01	6.6e−01	1.0e+00	9.9e−01	1.0e+00

C. BgBS90 − Unweighted UniFrac

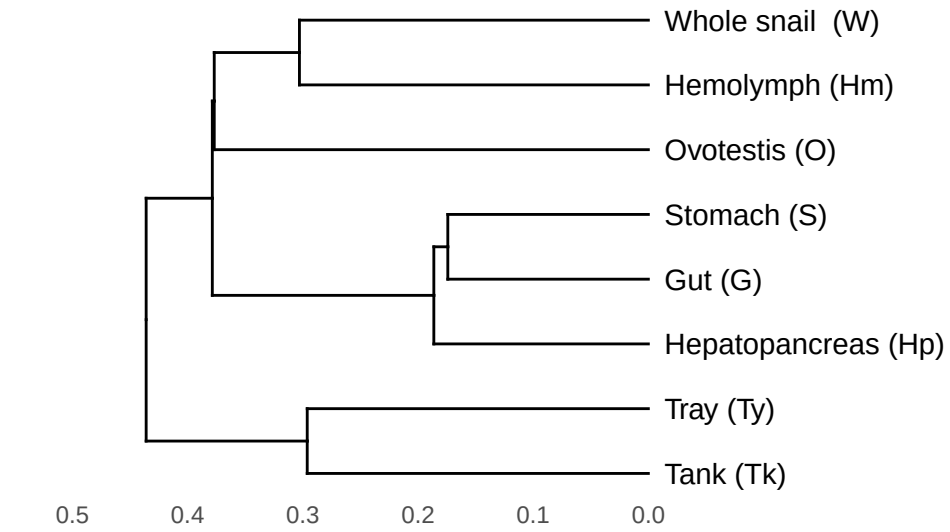

Permanova test \ β−dispersion test	Hm	S	G	Hp	O	W	Ty	Tk
Tk	5.6e−03	4.3e−03	4.0e−03	4.0e−03	4.3e−03	3.5e−02	2.4e−01	
Ty	4.0e−03	4.0e−03	4.3e−03	4.3e−03	5.6e−03	4.3e−02		9.2e−01
W	4.4e−02	6.2e−03	4.0e−03	1.2e−02	6.2e−03		9.0e−01	2.0e−01
O	2.7e−02	4.3e−03	4.0e−03	1.7e−02		1.0e−02	3.6e−01	9.9e−01
Hp	6.2e−03	3.4e−02	2.1e−02		9.9e−01	5.7e−02	7.8e−01	1.0e+00
G	4.3e−03	4.1e−01		1.0e+00	1.0e+00	3.9e−02	6.9e−01	1.0e+00
S	4.0e−03		1.0e+00	1.0e+00	9.0e−01	1.2e−01	9.2e−01	1.0e+00
Hm		1.0e+00	1.0e+00	1.0e+00	1.0e+00	3.4e−02	6.5e−01	1.0e+00

D. BgBS90 − Weighted UniFrac

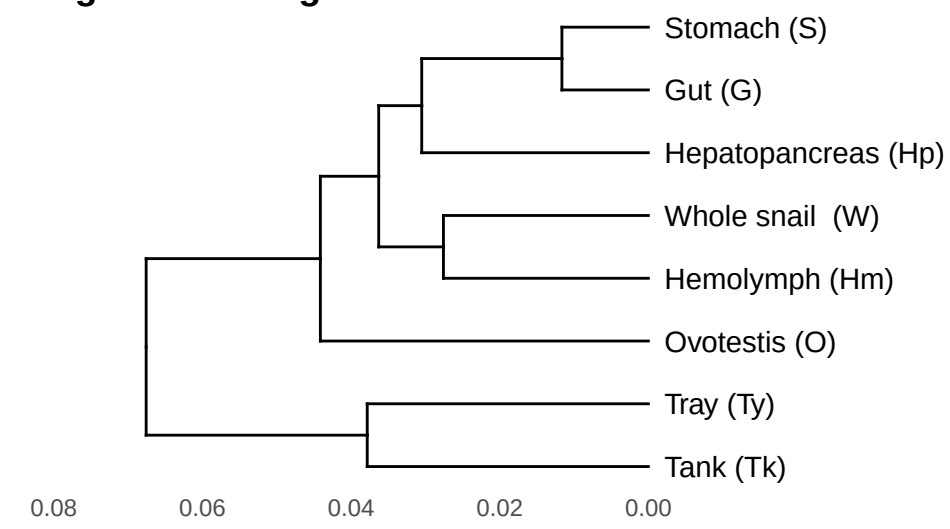

Permanova test \ β−dispersion test	Hm	S	G	Hp	O	W	Ty	Tk
Tk	2.8e−03	3.5e−03	2.8e−03	2.8e−03	2.8e−03	3.8e−02	6.5e−02	
Ty	2.8e−03	2.8e−03	3.5e−03	2.8e−03	3.5e−03	4.6e−02		1.0e+00
W	1.9e−01	9.3e−03	2.8e−03	3.5e−03	1.9e−02		1.0e+00	1.0e+00
O	3.5e−03	2.8e−03	2.8e−03	2.0e−02		1.0e+00	1.0e+00	1.0e+00
Hp	1.0e−01	3.5e−03	6.6e−03		1.0e+00	1.0e+00	1.0e+00	1.0e+00
G	1.3e−01	4.9e−01		1.0e+00	1.0e+00	9.9e−01	1.0e+00	1.0e+00
S	3.5e−02		1.0e+00	1.0e+00	1.0e+00	1.0e+00	1.0e+00	1.0e+00
Hm		1.0e+00	9.9e−01	1.0e+00	1.0e+00	1.0e+00	1.0e+00	1.0e+00

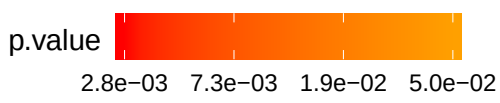

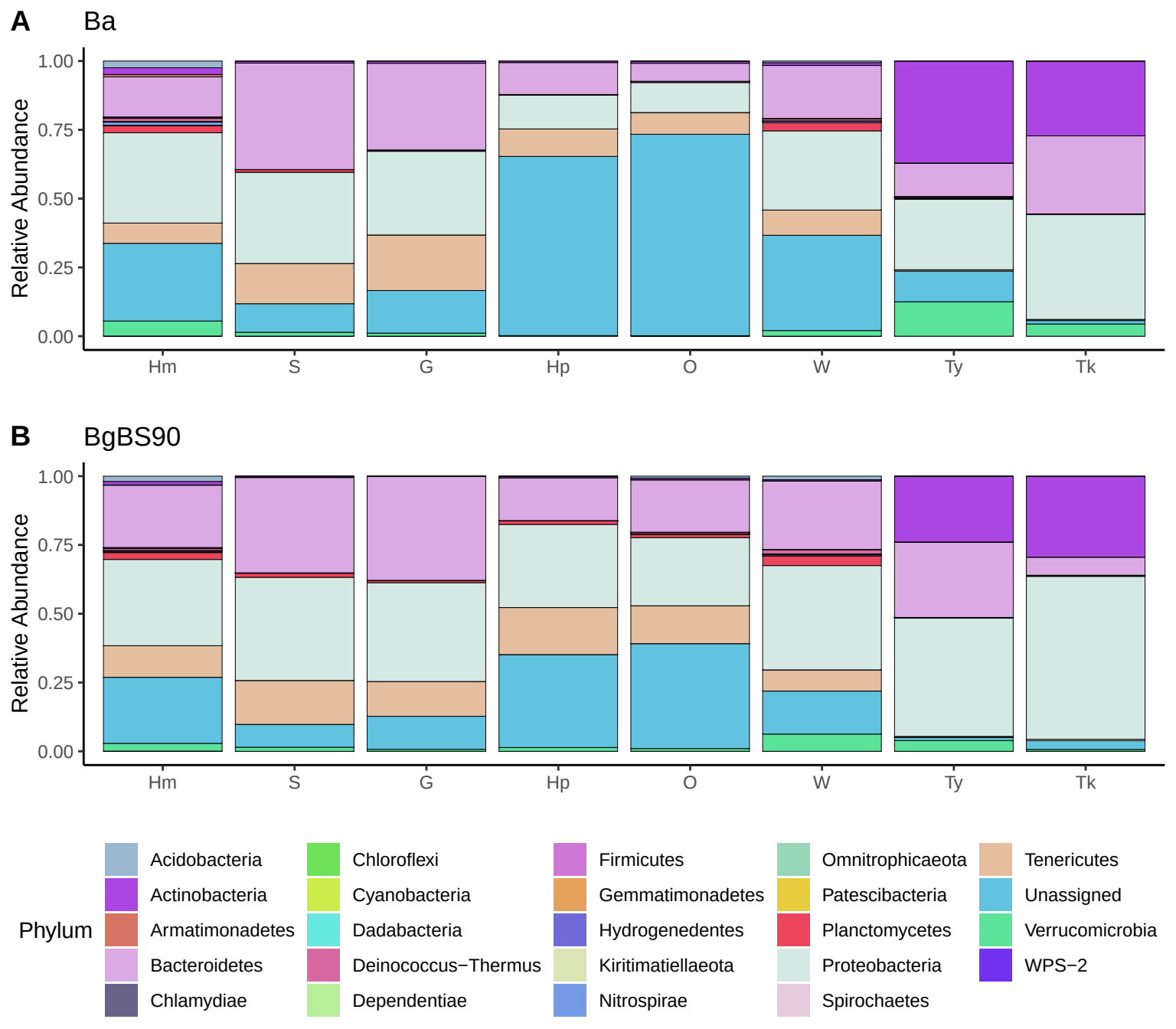
A
Ba
Relative Abundance
1.00
0.75
0.50
0.25
0.00
Hm
S
G
Hp
O
W
Ty
Tk
B
BgBS90
Relative Abundance
1.00
0.75
0.50
0.25
0.00
Hm
S
G
Hp
O
W
Ty
Tk
Phylum
Acidobacteria
Actinobacteria
Armatimonadetes
Bacteroidetes
Chlamydiae
Chloroflexi
Cyanobacteria
Dadabacteria
Deinococcus−Thermus
Dependentiae
Firmicutes
Gemmatimonadetes
Hydrogenedentes
Kiritimatiellaeota
Nitrospirae
Omnitrophicaeota
Patescibacteria
Planctomycetes
Proteobacteria
Spirochaetes
Tenericutes
Unassigned
Verrucomicrobia
WPS−2

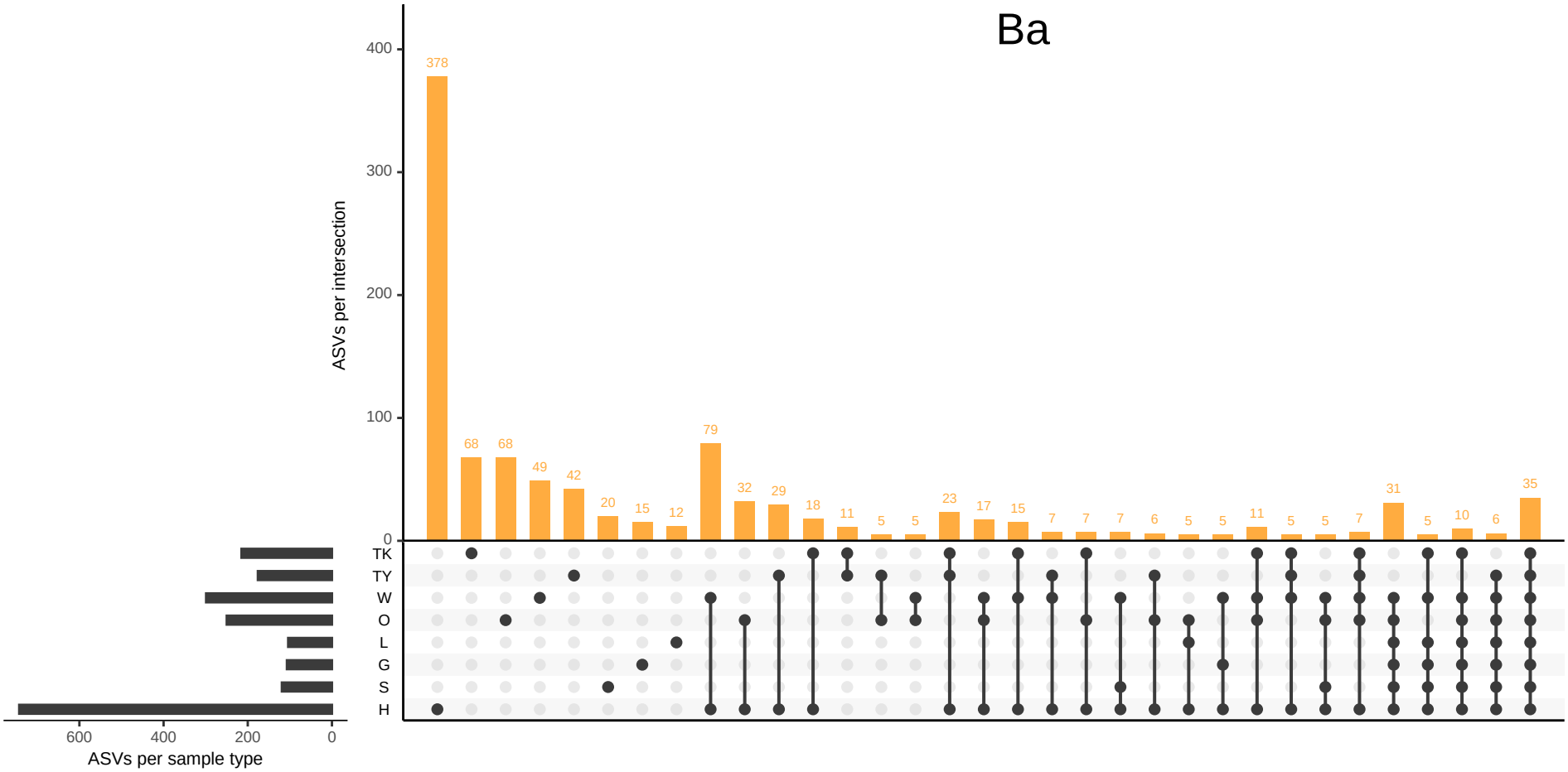
Ba
ASVs per intersection
0
100
200
300
400
378
68
68
49
42
20
15
12
79
32
29
18
11
5
5
23
17
15
7
7
7
6
5
5
11
5
5
7
31
5
10
6
35
TK
TY
W
O
L
G
S
H
600
400
200
0
ASVs per sample type

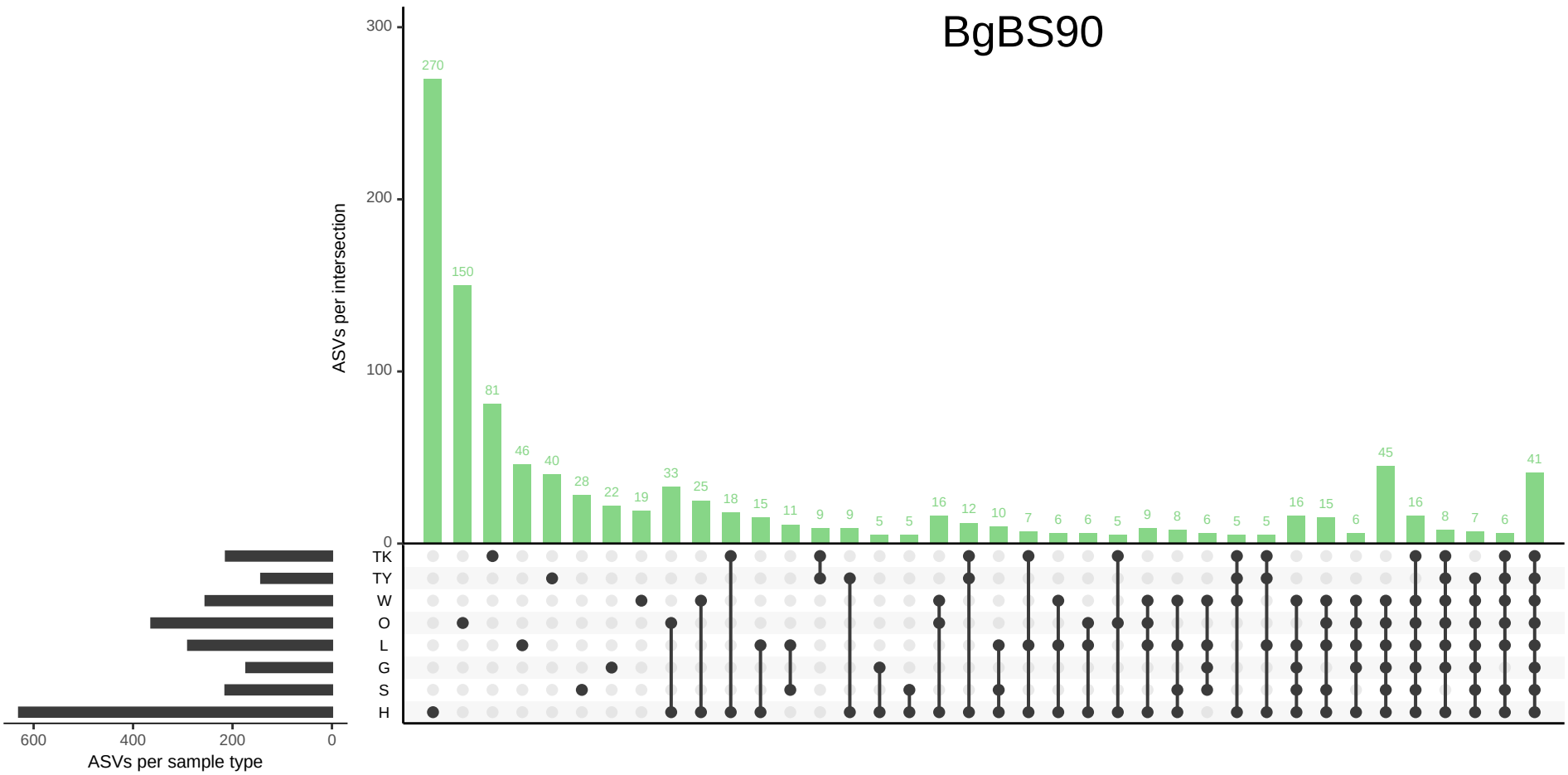
BgBS90
ASVs per intersection
0
100
200
300
270
150
81
46
40
28
22
19
33
25
18
15
11
9
9
5
5
16
12
10
7
6
6
5
9
8
6
5
5
16
15
6
45
16
8
7
6
41
TK
TY
W
O
L
G
S
H
600
400
200
0
ASVs per sample type

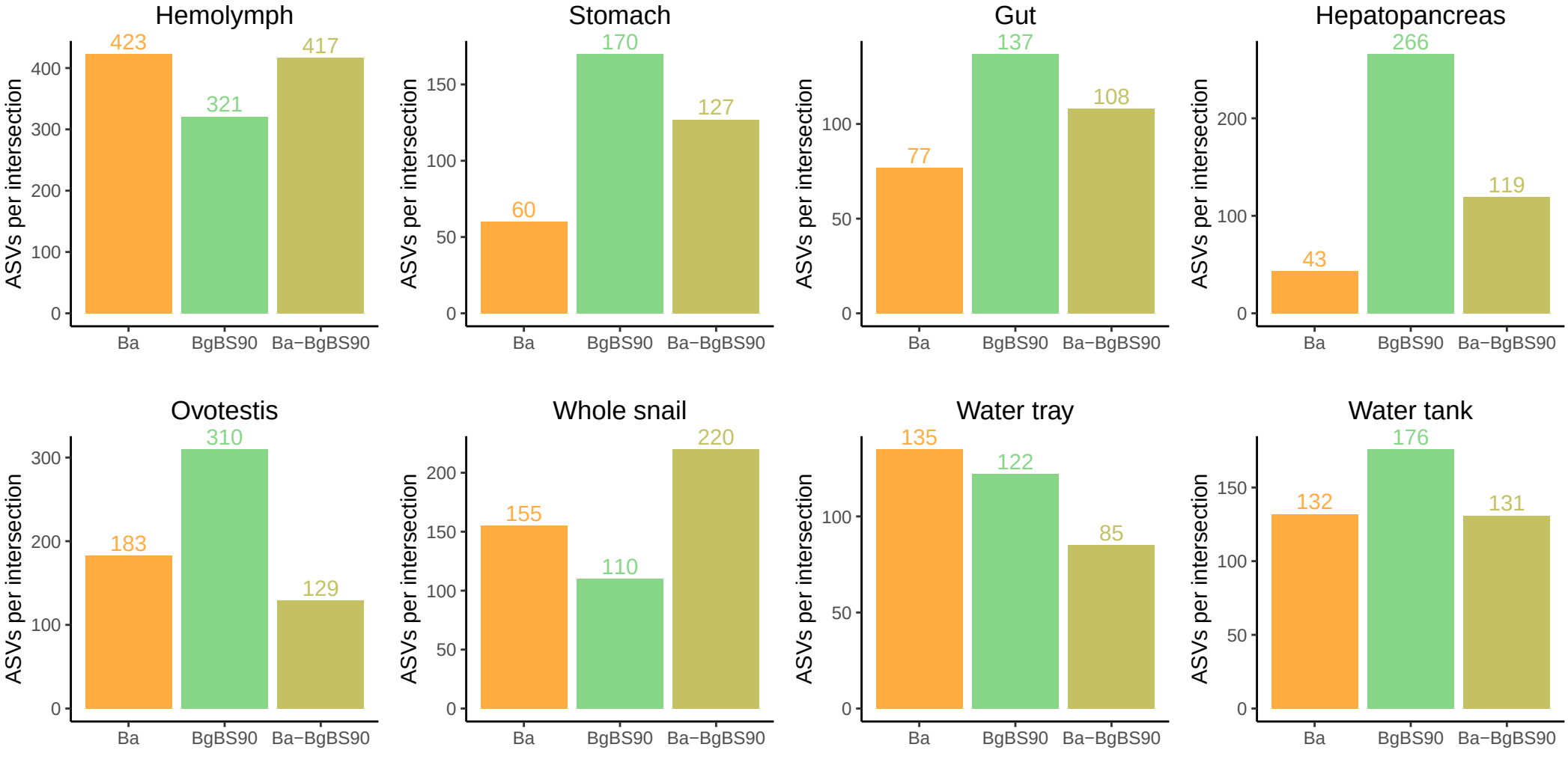
Hemolymph
423
321
417
Stomach
60
170
127
Gut
77
137
108
Hepatopancreas
43
266
119
Ovotestis
183
310
129
Whole snail
155
110
220
Water tray
135
122
85
Water tank
132
176
131
ASVs per intersection
Ba
BgBS90
Ba−BgBS90

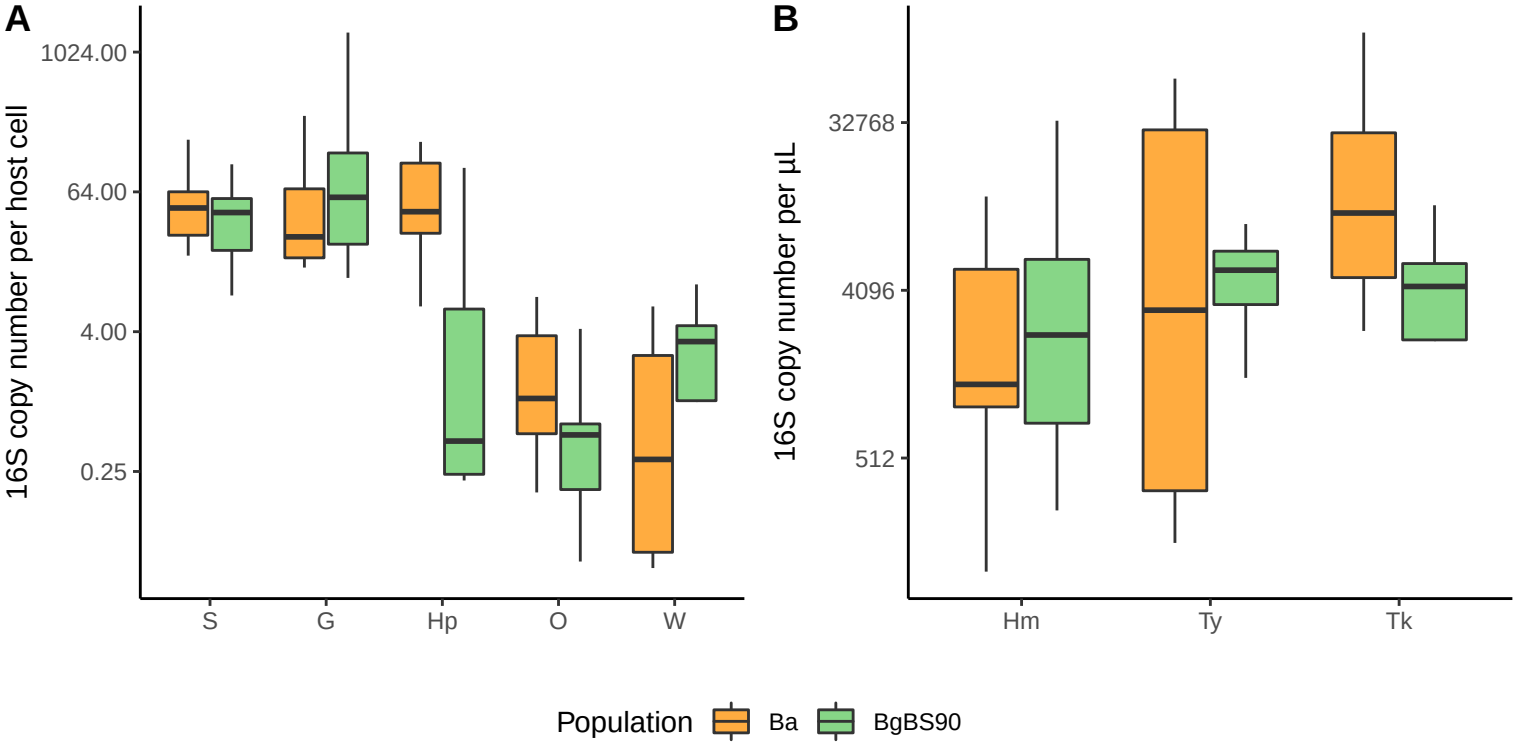
A
16S copy number per host cell
1024.00
64.00
4.00
0.25
S
G
Hp
O
W
B
16S copy number per µL
32768
4096
512
Hm
Ty
Tk
Population
Ba
BgBS90